Front. Phys., 2014, 9(2): 219–225
DOI 10.1007/s11467-013-0391-z

RESEARCH ARTICLE

# Concentration-dependent crystal structure, elastic constants and electronic structure of $Zr_xTi_{1-x}$ alloys under high pressure

**Xiao-Li Yuan**[1,2,4,*], **Mi-An Xue**[2,3], **Wen Chen**[1,2,†], **Tian-Qing An**[4]

[1] *College of Mechanics and Materials, Hohai University, Nanjing 210098, China*
[2] *State Key Laboratory of Hydrology-Water Resources and Hydraulic Engineering, Hohai University, Nanjing 210098, China*
[3] *College of Harbour Coastal and Offshore Engineering, Hohai University, Nanjing 210098, China*
[4] *College of Science, Hohai University, Nanjing 210098, China*
*Corresponding authors. E-mail: *yuanxiaoli0913@163.com, †chenwen@hhu.edu.cn*
*Received May 24, 2013; accepted September 6, 2013*

The physical properties of $Zr_xTi_{1-x}$ ($x = 0.0, 0.33, 0.5, 0.67, 0.75$ and $1.00$) alloys were simulated by virtual crystal approximation (VCA) methods which is generally used for disordered solid solutions modeling. The elastic constant, electronic structure and thermal Equation of state (EOS) of disordered $Zr_xTi_{1-x}$ alloys under pressure are investigated by plane-wave pseudo-potential method. Our simulations reveal increasement of variations of the calculated equilibrium volumes and decreasement of Bulk modulus as a function of the alloy compositions. Lattice parameters $a$ and $c$ of alloys with different Zr concentrations decrease linearly with pressure increasing, but the $c/a$values are increasing as pressure increases, indicating no phase transitions under pressure from 0 GPa to 100 GPa. The elastic constants and the Bulk modulus to the Shear modulus ratios ($B/G$) indicate good ductility of Zr, $Zr_{0.33}Ti_{0.67}$, $Zr_{0.5}Ti_{0.5}$, $Zr_{0.75}Ti_{0.25}$ and Ti, but the $Zr_{0.67}Ti_{0.33}$ alloy is brittle under 0 K and 0 GPa. The metallic behavior of these alloys was also proved by analyzing partial and total DOS.

**Keywords** dalloy, density functional theory, virtual crystal approximation (VCA), mechanics, elastic properties

**PACS numbers** 62.20.-x, 62.50.-p, 71.15.Mb, 71.20.Be

## 1 Introduction

Zirconium and titanium are members of the IVB group in the periodic table of elements, and are known to have similar structural and chemical properties. Zr and some of its alloys are widely used in the aerospace, nuclear, and biomedical industry [1–8] because of their high mechanical strength, stiffness, light density, and superior corrosion resistance than other alloys [9]. What's more, Ti alloys have been used as implant materials because of their excellent chemical and physical properties of relatively low elastic modulus, high strength-to-weight ratio, good fracture toughness, biocompatibility and superior corrosion resistance [10]. The narrow $d$-band in the midst of a broad $sp$-band of these materials is responsible for their stability, whereas a pressure-induced $s$–$d$ electron transfer leads to their structural and electronic transitions [11, 12].

Extensive theoretical calculations [13–17] and experimental studies [18–24] have been performed to study the phase transformation and mechanical properties of Ti and Zr. Bashkin [25–27] and Aksenenkov [28] have reported that the pressure for the $\alpha \rightarrow \omega$ transition of TiZr alloy is about 5–6 GPa at room temperature. Zirconium-tin alloys are also of practical crucial for nuclear industry. Partial substitution of Zr by Ti may control the properties of Zr alloys, particularly to reduce the weight of the parts of nuclear reactors. Because the Ti-Zr system is a complete solid solution with both the high temperature beta phase and the low temperature alpha phase [29], an extensive variation of alloy design is available. The structural and mechanical properties of a series of binary Ti-Zr alloys with Zr contents and Ti contents re-

spectively up to 40 wt.% had been evaluated [30, 31]. In addition to these studies, the mechanical properties and grindability of a binary Ti-Zr alloy containing different alloying elements (Nb, Mo, Cr and Fe) was also investigated [32]. Despite extensive experimental studies of the structural and mechanical properties of alloys with different Ti/Zr ratios [30–32], systematical first-principles calculations of the total energy and elastic constants of the disordered alloy behavior of Ti-Zr system has not yet been done, which is the aim of our work.

The virtual crystal approximation (VCA) method was employed to study the disordered alloys [33, 34]. Composite potential is constructed to represent the average of the component atoms comprising the inhomogeneity, the potentials which represent atoms of two or more elements are averaged into a composite atomic potential. In this work, we investigated the phase transition of $Zr_xTi_{1-x}$ alloys based on VCA and first-principle calculations, which has been successfully used to investigate mechanics and thermodynamic properties of metal material [35–40]. Properties of pure Zr and Ti, i.e., $x = 1$ and 0, were also calculated in order to compare with those of the alloys.

## 2 Computational methods

In our calculations, the electronic wave functions were expanded in a plane-wave basis set with an energy cut-off 530 eV. Pseudo-atomic calculations were performed for Zr ($4s^24p^64d^25s^2$) and Ti ($3s^23p^63d^24s^2$). As regards the Brillouin zone $k$-point sampling, $14 \times 14 \times 9$ Monkhorst–Pack meshes [41] were employed for the Hcp structure, which was enough to get the self-consistent convergence of the total energy to $10^{-6}$ eV/atom. The ultrasoft pseudopotentials introduced by Vanderbilt [42] were used to calculate all the ion–electron interactions. The effects of exchange-correlation interaction were treated by the generalized gradient approximation (GGA) [43] and the Perdew–Wang (PW) [44] formula. All of these calculations were conducted by the CASTEP package [45].

## 3 Results and discussion

### 3.1 Structure of alloys

In order to determine the theoretical equilibrium geometry, a series of different lattice parameters were used to calculate the total energy $E$ and the corresponding volume $V$ of Hcp $Zr_xTi_{1-x}$ ($x = 0.0, 0.33, 0.5, 0.67, 0.75$ and 1.00) alloys. According to the optimized lattice parameter ratio $c/a$ (for example $zr_{0.33}ti_{0.67}$) 1.585, we keep the ratio value ($c/a$) unchanged, a series of different values of lattice constants which change from 2.483 to 3.415 with a step of 0.068 are set to calculate the total energies $E$ and the corresponding volumes $V$, and then an energy–volume ($E-V$) curve can be obtained by fitting the calculated $E-V$ data to the Brich–Murnaghan of state (EOS). For other $Zr_xTi_{1-x}$, method ibid. Then the energy–volume ($E-V$) data were fitted with the four-order Birch–Murnaghan equation of state (EOS) [46]. The calculated equilibrium volume $V_0$ and Bulk modulus $B_0$ of the alloys as a function of the Zr concentration ($x$) as well as the experimental and theoretical data of pure Zr [47–49] and Ti [50–52] are shown in Fig. 1. The equilibrium volume $V_0$ decreases whereas the Bulk modulus $B_0$ increases along with the increase of the Zr concentration. Our results for pure Zr and Ti are highly consistent with the experimental data. The obtained $V_0$ and $B_0$ of the $Zr_xTi_{1-x}$ alloys as a function of the Zr concentration can be well described by forth-order polynomials:

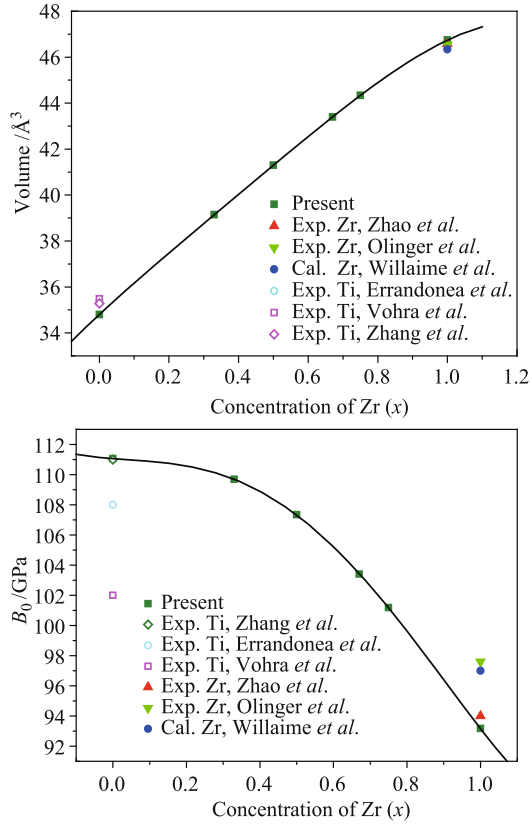


**Fig. 1** Equilibrium structural parameters $V_0$ and $B_0$ of Hcp $Zr_xTi_{1-x}$ are shown as a function of the Zr concentration. The VCA results are shown by solid squares and circles. The experimental data [47, 48] and the computational data [49] of pure Zr, are shown by solid delta gradient and solid circles, respectively; whereas the experimental data of pure Ti is shown by open circles, squares and diamonds [50–52]; the solid lines are the fitted data according to VCA results.

$$V_0 = 34.80377 + 14.08015X - 4.9751X^2 + 8.29203X^3 - 5.45781X^4 \quad (1)$$

$$B_0 = 111.05623 - 1.87514X + 5.58687X^2 - 45.47828X^3 + 23.88087X^4 \quad (2)$$

The $Zr_xTi_{1-x}$ alloys structure was optimized under compression. The predicted static EOS ($P-V$) data as well as the experimental values of pure Zr [47–49] and Ti [50–52] are shown in Fig. 2. It is found from Fig. 2 that the calculated results and the experimental results are highly agreement. The volume of $Zr_xTi_{1-x}$ alloys decreases along with the increase of pressure, and the volume decreases along with the increase of pressure much more slowly under high Zr concentration, implying smaller compression under high Zr concentration and stronger electron exclusive interactions between Zr than Ti. Figure 3 shows the calculated lattice parameters $a$ and $c$ as a function of pressure as well as the experimental and theoretical values of pure Zr [47–49] and Ti [50–52]. The lattice parameter $a$linearly decreases along with the increase of pressure. The lattice parameter $c$ first decreases and then increases when the pressure increases. It is noted that the value of $c$ increases from 80 GPa to 100 GPa when $x = 0$ and 0.75, and the value of $c$ at 90 GPa is larger than that at 80 GPa with $x = 0.67$. The reasons of these phenomena are possible that zirconium and titanium atoms in the Hcp structure arrange in different ways. Titanium atoms along the $a$-axis direction are many and zirconium atoms along the $c$-axis direction are much more, the mutual exclusion forces between Ti and Ti atoms are less than those between Zr and Zr atoms. With the increase of pressure, their volumes are decreasing and the effect of pressure on volume becomes much small. However, visible jump point is not found, which implies no phase transition when pressure changes from 0 GPa to 100 GPa. As shown in Fig. 4, the lattice parameter ratio ($c/a$) gradually increases with the increase of pressure, without jump point, indicating no phase transition. This result is also consistent with the conclusion that the lattice parameters $a$ and $c$ depend on pressure.

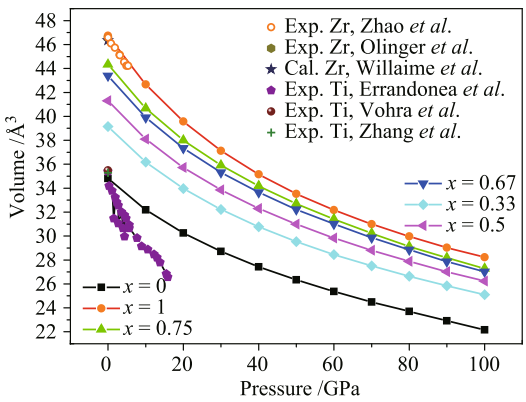


**Fig. 2** The $P-V$ relationship for Hcp $Zr_xTi_{1-x}$ together with the experimental [47, 48] and theoretical [49] data of pure Zr or pure Ti [50–52].

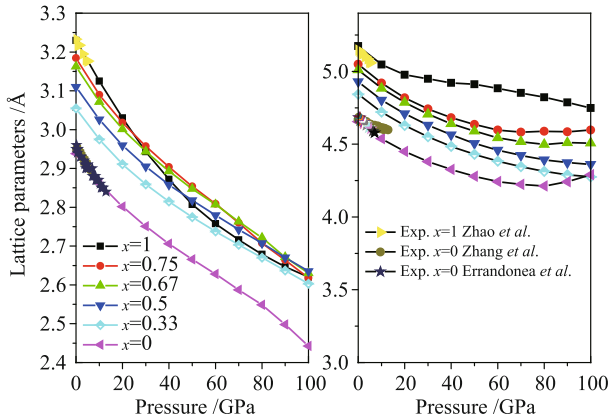


**Fig. 3** Lattice constants $a$ and $c$ of $Zr_xTi_{1-x}$ as a function of pressure.

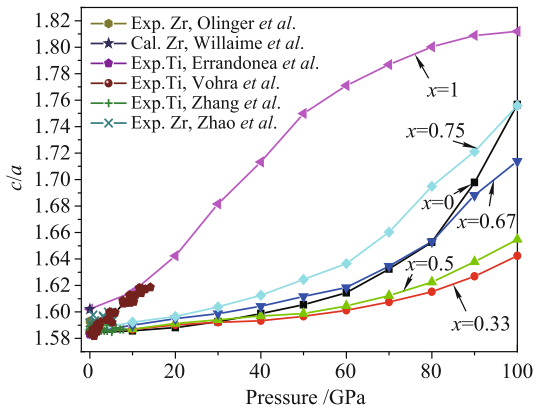


**Fig. 4** The $c/a$ axial ratio of $Zr_xTi_{1-x}$ as a function of pressure.

### 3.2 Elastic properties

The elastic constant is a physical quantity, which represents the elastic strength and many mechanical properties of solid materials such as Young's modulus, Bulk modulus and Shear modulus. It could also be used to explore the interaction forces between atoms [53, 54]. Therefore, studies of elastic properties of solid materials not only play a vital role in the area of basic scientific research, but are also important for practical engineering. In our studies, we calculated the elastic constants of the $Zr_xTi_{1-x}$ alloys with different Zr concentrations under 0 GPa and 50 GPa, and the results are shown in Fig. 5. The elastic constant values $c_{11}, c_{33}, c_{12}$ and $c_{13}$ under 50 GPa are all larger than those under 0 GPa except for $c_{44}$, implying that compression along $c_{44}$ under high pressure is much more difficult than $c_{11}$, $c_{33}$, $c_{12}$ and $c_{13}$.

The changes of $c_{11}$ and $c_{12}$ values along with the Zr concentrations are larger than $c_{33}$ and $c_{44}$ under 0 GPa and 50 GPa.

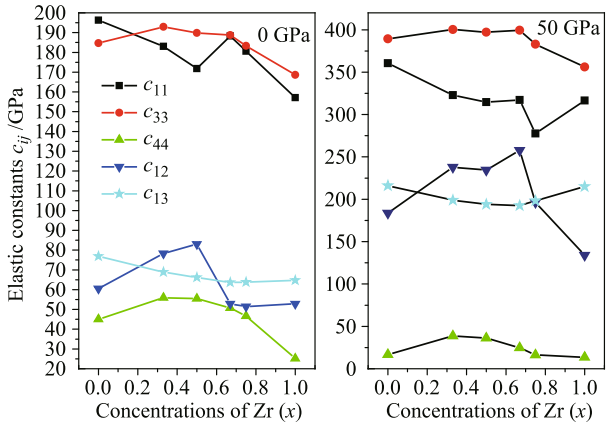


**Fig. 5** Elastic constants of $Zr_xTi_{1-x}$ alloys with different Zr concentrations under 0 GPa and 50 GPa, respectively.

Elastic modulus represents the resistance to forces and the elastic deformation under external forces. Therefore, it is an important quantity to describe material mechanical properties. It is also a very important physical quantity describing the interactions between atoms in crystals and the strength of atomic bonding forces. In our simulations, the Bulk modulus and Shear modulus of $Zr_xTi_{1-x}$ alloys are calculated. Pugh [55] proposed an empirically method to predict the ductile and brittle behavior of solids based on elastic modulus by calculating the $r = B/G$ ration. If $r < 1.75$, the solid behaves in a brittle manner, otherwise in a ductile manner. Figure 6 shows the ratios of Bulk modulus to Shear modulus $(B/G)$ as a function of pressure. The $(B/G)$ values of $Zr_xTi_{1-x}$ alloys ($x = 0.0, 0.33, 0.5, 0.67, 0.75$ and $1.00$) are 2.04, 1.98, 2.07, 1.74, 1.81 and 2.45, respectively. These values are larger than 1.75 except for that of the $Zr_{0.67}Ti_{0.33}$ which is 1.74. These results indicate that Zr, $Zr_{0.33}Ti_{0.67}$, $Zr_{0.5}Ti_{0.5}$, $Zr_{0.75}Ti_{0.25}$ and Ti behave in a ductile manner under 0 GPa and 0 K while the $Zr_{0.67}Ti_{0.33}$ alloy is brittle, and its the brittleness changes into the ductility as the pressure increases. The physical reason of the phenomenon could be related to the atomic and electronic distributions as well as the interaction between atoms and electrons. Moreover, the ductility of these six alloys increases along with the increase of pressure, implying improvement of their ductility by increasing pressure.

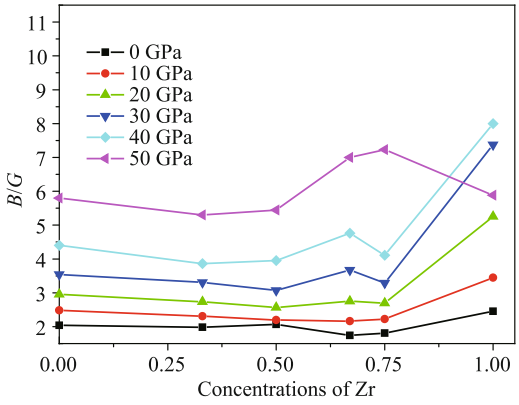


**Fig. 6** The $B/G$ values of $Zr_xTi_{1-x}$ with different Zr concentration under different pressure.

### 3.3 Electronic structure

Zirconium and titanium are transition metal, and they are not full of shell $d$-orbit, a narrow $d$-band in the midst of abroad $sp$-band, so they exhibit the peculiar physical properties different from other metallic materials. The $d$-band occupancy is crucial for the structural and electronic properties of solid materials, whereas the pressure induced $s$–$d$ electron transfer plays an important role in the structural stability of solid materials [56]. Therefore, in order to better understand interactions and structures of micro-electronics in the zirconium-titanium alloy, we calculated the electronic structures of six different alloys including titanium, $Zr_{0.33}Ti_{0.67}$, $Zr_{0.5}Ti_{0.5}$, $Zr_{0.75}Ti_{0.25}$, $Zr_{0.67}Ti_{0.33}$ and zirconium under high pressure. The total density of states (DOS) and partial density of states of alloys with different components around the Fermi level $(E_f)$ are shown in Fig. 7. The total density of states reached their maximum when $x = 0.75$, and it is seen from the partial density of states that $d$ electronic contribution near the Fermi surface $(E_f)$ is larger and $d$ electronic contribution becomes smaller and smaller as away

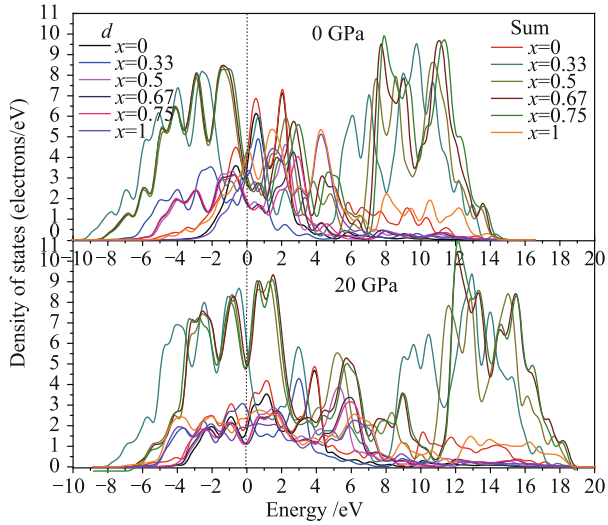


**Fig. 7** Total and partial ($d$ electron) densities of state of Zr-Ti alloy at 0 GPa and 20 GPa, respectively. The different styles of the lines represent the results of alloys with different Zr concentrations.

from the Fermi surface ($E_f$) under 0 GPa. Under 20 GPa, the strength of total density of states was all enhanced, whereas the*d* electronic contribution was relatively reduced. The total density of states moved to high energy region. That is to say, the Fermi surface ($E_f$) moved down relative to the Fermi surface ($E_f$) under 0 GPa, which indicates the nature of metal is enhanced under pressure.

## 4 Conclusion

In this paper, we studied structure, elastic constants, electronic structure and thermal EOS of the disordered $Zr_xTi_{1-x}$ alloys including Zr, $Zr_{0.33}Ti_{0.67}$, $Zr_{0.5}Ti_{0.5}$, $Zr_{0.75}Ti_{0.25}$, $Zr_{0.67}Ti_{0.33}$ and Ti under high pressure by using first principle calculations and the virtual crystal approximation (VCA) method. The lattice parameters of alloys with different Zr concentrations decrease, whereas the ratio of these lattice parameters ($c/a$) increases along with the increase of pressure without obvious hop, implying no phase transition under pressure from 0 GPa to 100 GPa. The values of $B/G$ indicated that Zr, $Zr_{0.33}Ti_{0.67}$, $Zr_{0.5}Ti_{0.5}$, $Zr_{0.75}Ti_{0.25}$ and Ti have excellent ductility but $Zr_{0.67}Ti_{0.33}$ is brittle under 0 GPa and 0 K. The ductility of these six compounds increases along with the increase of pressure, implying improvement of the ductility under high pressure. Electronic structure calculations revealed the highest intensity of total density of states is for the $Zr_{0.75}Ti_{0.25}$ alloy and partial density of states *d* electrons contribute the most under 0 GPa. The intensity of the total density of States increase and Fermi surface moves down along with the increase of the pressure and the nature of metal of the alloys is enhanced under 20 GPa.

**Acknowledgements** The first author greatly thanks Dr. Ruo-Xu Gu for his help with English language editing. The work was supported by Postdoctoral Science Foundation of China (Grant No. 2013M541596), Jiangsu Planned Projects for Postdoctoral Research Funds (Grant No. 1202105C), National Basic Research Program of China (Grant No. 2010CB731600), the National Natural Science Foundation of China (Grant Nos. 51209080, 10776022, and 20773085), China Academy of Engineering Physics (CAEP), and China Postdoctoral Science Foundation funded project (Grant No. 2012M511192).

## References

1. Y. Okazaki, S. Rao, T. Tateishi, and Y. Ito, Cytocompatibility of various metal and development of new titanium alloys for medical implants, *Mat. Sci. Eng. A*, 1998, 243(1–2): 250
2. M. Niinomi, Fatigue performance and cyto-toxicity of low rigidity titanium alloy, Ti-29Nb-13Ta-4.6Zr, *Biomaterials*, 2003, 24: 2673
3. Y. Okazaki, S. Asao, S. Rao, and T. Tateishi, Effect of concentration of Zr, Sn, Nb, Ta, Pd, Mo, Co, Cr, Si, Ni, Fe on the relative growth ratios of bio-cells, *J. Jpn. Inst. Met.*, 1996, 60: 902
4. D. L. Douglass, The physical metallurgy of zirconium, *At. Energy Rev.*, 1963, 3: 71
5. H. Ikehata, N. Nagasako, T. Furuta, A. Fukumoto, K. Miwa, and T. Saito, First-principles calculations for development of low elastic modulus Ti alloys, *Phys. Rev. B*, 2004, 70(17): 174113
6. W. Liu, B. Li, L. Wang, J. Zhang, and Y. Zhao, Elasticity of w-phase zirconium, *Phys. Rev. B*, 2007, 76(14): 144107
7. M. T. Pérez-Prado and A. P. Zhilyaev, First experimental observation of shear induced hcp to bcc transformation in pure Zr, *Phys. Rev. Lett.*, 2009, 102(17): 175504
8. L. Saldana, A. Méndez-Vilas, L. Jiang, M. Multigner, J. L. González-Carrasco, M. T. Pérez-Prado, M. L. González-Martín, L. Munuera, and N. Vilaboa, In vitro biocompatibility of an ultrafine grained zirconium, *Biomaterials*, 2007, 28(30): 4343
9. N. Stojilovic, E. T. Bender, and R. D. Ramsier, Surface chemistry of zirconium, *Prog. Surf. Sci.*, 2005, 78(3–4): 101
10. M. Long and H. J. Rack, Titanium alloys in total joint replacement-a materials science perspective, *Biomaterials*, 1998, 19(18): 1621
11. J. C. Duthie and D. G. Pettifor, Correlation between d-band occupancy and crystal structure in the rare earths, *Phys. Rev. Lett.*, 1977, 38(10): 564
12. H. L. Skriver, Crystal structure from one-electron theory, *Phys. Rev. B*, 1985, 31(4): 1909
13. Z. G. Mei, S. L. Shang, Y. Wang, and Z. K. Liu, Density-functional study of the pressure-induced phase transitions in Ti at zero Kelvin, *Phys. Rev. B*, 2009, 79(13): 134102
14. C. E. Hu, Z. Y. Zeng, L. Zhang, X. R. Chen, L. C. Cai, and D. Alfè, Theoretical investigation of the high pressure structure, lattice dynamics, phase transition, and thermal equation of state of titanium metal, *J. Appl. Phys.*, 2010, 107(9): 093509
15. Y. J. Hao, L. Zhang, X. R. Chen, L. C. Cai, Q. Wu, and D. Alfè, *Ab initio* calculations of the thermodynamics and phase diagram of zirconium, *Phys. Rev. B*, 2008, 78(13): 134101
16. I. Schnell and R. C. Albers, Zirconium under pressure: Phase transitions and thermodynamics, *J. Phys.: Condens. Matter*, 2006, 18(5): 1483
17. R. Ahuja, J. M. Wills, B. Johansson, and O. Eriksson, Crystal structures of Ti, Zr, and Hf under compression: Theory, *Phys. Rev. B*, 1993, 48(22): 16269
18. H. Xia, S. J. Duclos, A. L. Ruoff, and Y. K. Vohra, New high-pressure phase transition in zirconium metal, *Phys. Rev. Lett.*, 1990, 64(2): 204

19. H. Xia, A. L. Ruoff, and Y. K. Vohra, Temperature dependence of the w-bcc phase transition in zirconium metal, *Phys. Rev. B*, 1991, 44(18): 10374
20. Y. Akahama, M. Kobayashi, and H. Kawamura, Superconductivity and phase transition of zirconium under high pressure up to 50 GPa, *J. Phys. Soc. Jpn.*, 1990, 59(11): 3843
21. Y. Akahama, M. Kobayashi, and H. Kawamura, High-pressure X-ray diffraction study on electronics-d transition in zirconium, *J. Phys. Soc. Jpn.*, 1991, 60(10): 3211
22. Y. Akahama, H. Kawamura, and T. LeBihan, New d (distorted-bcc) titanium to 220 GPa, *Phys. Rev. Lett.*, 2001, 87(27): 275503
23. Y. S. Zhao and J. Z. Zhang, Enhancement of yield strength in zirconium metal through high-pressure induced structural phase transition, *Appl. Phys. Lett.*, 2007, 91(20): 201907
24. Y. K. Vohra and P. T. Spencer, Novel g-phase of titanium metal at megabar pressures, *Phys. Rev. Lett.*, 2001, 86(14): 3068
25. I. O. Bashkin, A. Yu. Pagnuev, A. F. Gurov, V. K. Fedotov, G. E. Abrosimova, and E. G. Ponyatovskii, Phase transformations in equiatomic alloy TiZr at pressure up to 70 kbar, *Phys. Solid State*, 2000, 42(1): 170
26. I. O. Bashkin, A. Yu. Pagnuev, A. F. Gurov, V. K. Fedotov, G. E. Abrosimova, and E. G. Ponyatovsky, Enhanced superconductivity of the Ti-Zr alloys in the high-pressure BCC phase, *JETP Lett.*, 2001, 73(2): 75
27. I. O. Bashkin, V. K. Fedotov, M. V. Nefedova, V. G. Tissen, E. G. Ponyatovsky, A. Schiwek, and W. B. Holzapfel, Crystal structure and superconductivity of TiZr up to 57 GPa, *Phys. Rev. B*, 2003, 68(5): 054401
28. V. V. Aksenenkov, V. D. Blank, B. A. Kulnitskiy, and E. I. Estrin, *Phys. Met. Metalloved.*, 1990, 69: 154
29. J. L. Murray, Phase Diagrams of Binary Titanium Alloys, ASM International, Materials Park, OH, 1987: 340
30. W. F. Ho, W. K. Chen, S. C. Wu, and H. C. Hsu, Structure, mechanical properties, and grindability of dental Ti-Zr alloys, *J. Mater. Sci. Mater. Med.*, 2008, 19(10): 3179
31. H. C. Hsu, S. C. Wu, Y. C. Sung, and W. F. Hod, The structure and mechanical properties of as-cast Zr-Ti alloys, *J. Alloy. Comp.*, 2009, 488(1): 279
32. W. F. Ho, C. H. Cheng, C. H. Pan, S. C. Wu, and H. C. Hsu, Structure, mechanical properties and grindability of dental Ti-10Zr-X alloys, *Mater. Sci. Eng. C*, 2009, 29(1): 36
33. T. Muto, On the electronic structure of alloys, *Sci. Pap. Inst. Phys. Chem. Res.*, 1938, 34: 377
34. L. Nørdheim, Zur Elektronentheorie der Metalle (I), *Ann. Phys.*, 1931, 9: 607
35. L. L. Sun, Y. Cheng, and G. F. Ji, Elastic and optical properties of $CeO_2$ via first-principles calculations, *J. At. Mol. Sci.*, 2010, 1: 143
36. X. L. Yuan, D. Q. Wei, X. R. Chen, Q. M. Zhang, and Z. Z. Gong, The first-principles calculations for the elastic properties of $Zr_2Al$ under compression, *J. Alloy. Comp.*, 2011, 509(3): 769
37. X. L. Yuan, D. Q. Wei, Y. Cheng, J. G. Fu, Q. M. Zhang, and Z. Z. Gong, Pressure effects on elastic and thermodynamic properties of $Zr_3Al$ intermetallic compound, *Comput. Mater. Sci.*, 2012, 58: 125
38. X. L. Yuan, D. Q. Wei, Y. Cheng, Q. M. Zhang, and Z. Z. Gong, Thermodynamic properties of $Zr_2Al$ under high pressure from first-principles calculations, *J. At. Mol. Sci.*, 2012, 3: 160
39. X. L. Yuan, M. A. Xue, W. Chen, T. Q. An, and Y. Cheng, Investigations on the structural, elastic and electronic properties of the orthorhombic Zirconium-Nickel alloy under different pressure, *Comput. Mater. Sci.*, 2012, 65: 127
40. X. R. Chen, Z. Y. Zeng, Z. L. Liu, L. C. Cai, and F. Q. Jing, Elastic anisotropy of $\varepsilon$-Fe under conditions at the Earth's inner core, *Phys. Rev. B*, 2011, 83(13): 132102
41. H. J. Monkhorst and J. D. Pack, Special points for Brillouin-zone integrations, *Phys. Rev. B*, 1976, 13(12): 5188
42. D. Vanderbilt, Soft self-consistent pseudopotentials in a generalized eigenvalue formalism, *Phys. Rev. B*, 1990, 41(11): 7892
43. B. Hammer, L. B. Hansen, and J. K. Norskov, Improved adsorption energetics within density-functional theory using revised Perdew–Burke–Ernzerhof functionals, *Phys. Rev. B*, 1999, 59(11): 7413
44. J. P. Perdew and Y. Wang, Accurate and simple analytic representation of the electron-gas correlation energy, *Phys. Rev. B*, 1992, 45(23): 13244
45. M. D. Segall, P. J. D. Lindan, M. J. Probert, C. J. Pickard, P. J. Hasnip, S. J. Clark, and M. C. Payne, First-principles simulation: ideas, illustrations and the CASTEP code, *J. Phys.: Condens. Matter*, 2002, 14(11): 2717
46. F. Birch, Finite elastic strain of cubic crystals, *Phys. Rev.*, 1947, 71(11): 809
47. Y. Zhao, J. Zhang, C. Pantea, J. Qian, L. L. Daemen, P. A. Rigg, R. S. Hixson, G. T. Gray, Y. Yang, L. Wang, Y. Wang, and T. Uchida, Thermal equations of state of the a, b, and w phases of zirconium, *Phys. Rev. B*, 2005, 71(18): 184119
48. B. Olinger and J. C. Jamieson, Zirconium: Phases and compressibility to 120 kilobars, *High Temp. High Press.*, 1973, 5: 123
49. F. Willaime and C. Massobrio, Development of an $N$-body interatomic potential for hcp and bcc zirconium, *Phys. Rev. B*, 1991, 43(14): 11653
50. D. Errandonea, Y. Meng, M. Somayazulu, and D. Hausermann, Pressure-induced $\alpha \rightarrow \omega$ transition in titanium metal: A systematic study of the effects of uniaxial stress, *Physica B*, 2005, 355(1–4): 116
51. Y. K. Vohra and P. T. Spencer, Novel $g$-phase of titanium metal at megabar pressures, *Phys. Rev. Lett.*, 2001, 86(14): 3068
52. J. Zhang, Y. Zhao, R. S. Hixson, G. T. Gray, L. P. Wang, W. Utsumi, S. Hiroyuki, and H. Takanori, Thermal equations of

state for titanium obtained by high pressure-temperature diffraction studies, *Phys. Rev. B*, 2008, 78(5): 054119

53. J. P. Poirier, Introduction to the Physics of the Earth's Interior, New York: Cambridge University Press, 1991
54. X. W. Sun, Q. F. Chen, X. R. Chen, L. C. Cai, and F. Q. Jing, First-principles investigations of elastic stability and electronic structure of cubic platinum carbide under pressure, *J. Appl. Phys.*, 2011, 110(10): 103507
55. S. F. Pugh, XCII. Relations between the elastic moduli and the plastic properties of polycrystaline pure metals, *Philos. Mag.*, 1954, 45: 823
56. H. L. Skriver, Crystal structure from one-electron theory, *Phys. Rev. B*, 1985, 31(4): 1909